

Ab-initio Phonon Calculations for the layered compound TiOCl

Leonardo Pisani and Roser Valentí

Institut für Theoretische Physik, Universität Frankfurt, D-60054 Frankfurt, Germany

(Dated: September 20, 2018)

We present first-principles frozen-phonon calculations for the three Raman-active A_g modes in the spin-1/2 layered TiOCl system within two different well-known approaches: the local density approximation (LDA) and the so-called LDA+U approximation. We observe that the inclusion of electron correlation in a mean-field level as implemented in the LDA+U leads to a better overall agreement with experimental results. We also discuss the implications of the two approaches on the physics of TiOCl.

PACS numbers: 75.30.Gw, 75.10.Jm, 78.30.-j

Introduction.- The layered quantum spin system TiOCl has been recently a subject of debate due to its anomalous properties at moderate to low temperatures. Susceptibility measurements¹ show a kink at $T_{c2}=94$ K and an exponential drop at $T_{c1}=66$ K indicating the opening of a spin gap which has been interpreted as a spin-Peierls phase transition¹. LDA+U calculations performed by these authors predicted the system to behave as a spin-chain along the b axis. X-ray diffraction measurements below $T_{c1}=66$ K report² the presence of superlattice reflections at $(h, k + 1/2, l)$ which denotes a doubling of the unit cell along the b axis and has been interpreted as a confirmation that the system undergoes a spin-Peierls phase transition below T_{c1} . Still unresolved is the nature of the kink at T_{c2} . The observation in Raman and infrared spectroscopy of phonon anomalies³ above T_{c2} as well as temperature-dependent g-factors and linewidths in ESR⁴ led to the proposal that the system is subject to competing lattice, spin, and orbital degrees of freedom. Recent heat capacity measurements⁵ seem to strongly support the idea of existence of possible lattice and/or orbital fluctuations above T_{c2} .

In view of the above discussion, it is of great importance to understand the behavior of the phonons in this system as well as the possibility of coupling to orbital and spin degrees of freedom. In a previous communication⁶ we presented first-principles results on the electronic properties of a few slightly distorted structures for TiOCl according to the various A_g -Raman active phonon modes expected for the $Pmmn$ space group assigned to TiOCl. The idea in ref.⁶ was to investigate the orbital occupancy as a function of lattice distortion, which could simulate the phonon-orbital interaction. The phonon modes and the corresponding eigenvectors in ref.⁶ were obtained by considering a shell model⁷.

In the present work, we abandon the parametrized procedure implicit in the shell model and we calculate the Raman-active A_g phonon modes in TiOCl within a first principles frozen phonon approach. From group theoretical analysis, the allowed A_g modes in the $Pmmn$ symmetry define ion displacements along the c -axis of the crystal. One important result of our calculations is that the consideration of correlations in this system is of crucial importance in order to get an accurate description of the phonons.

First Principles Frozen Phonon approach.- In order to calculate phonon frequencies within an *ab initio* scheme, two different methods are generally employed: the *energy surface* method⁸ and the *atomic force* method⁹. Within both methods the harmonic potentials underlying the lattice vibrations are constructed by selecting frozen-in distorted structures and then performing a Density Functional Theory (DFT) band-structure calculation. While in the first approach, energy values are needed to fit the energy surface to a bilinear form, in the second approach the atomic forces acting on the displaced ions are computed to fit the harmonic forces.

In both methods the corresponding dynamical matrix is calculated according to the following procedure. Within the Born-Oppenheimer approximation, the electronic energy hypersurface is represented as a function of the titanium, oxygen and chlorine coordinates along the c -axis. For small atomic displacements we approximate the surface by a Taylor expansion up to second order around its minimum (harmonic approximation). Since the minimum satisfies the equilibrium condition, the surface is described by the following bilinear form:

$$E - E_0 = \frac{1}{2} \sum_{ij} z_i K_{ij} z_j, \quad i, j = 1, 2, 3 \quad (1)$$

where z_i are the c -axis coordinates of the ions ($1 \equiv$ titanium, $2 \equiv$ oxygen, $3 \equiv$ chlorine). The equation of motion for the i -th atom with mass M_i is then

$$M_i \frac{d^2 z_i}{dt^2} = - \frac{\partial E}{\partial z_i} = - \sum_j K_{ij} z_j. \quad (2)$$

Seeking for running-wave solutions of the form: $z_i(t) = \frac{\xi_i}{\sqrt{M_i}} e^{-i\omega t}$ we are left with the eigenvalue problem $\omega^2 \xi_i = \sum_j \frac{K_{ij}}{\sqrt{M_i M_j}} \xi_j$ where the matrix $D_{ij} = \frac{K_{ij}}{\sqrt{M_i M_j}}$ is the well-known dynamical matrix.

Within the energy surface method, Eq. 1 is exploited to obtain the matrix D_{ij} , while within the atomic force method, the left-hand side of Eq. 2 is used.

In this work we will make use of both methods within two different approximated forms for the exchange-correlation potential in the DFT scheme, namely, the Local Density Approximation (LDA)¹⁰ and the so-called

LDA+ U approximation¹¹. For the LDA+ U calculations, we considered the implementation, E^U proposed by M.T.Czyzyk and G.A.Sawatzky¹² (named in the literature "AMF", Around Mean Field) which differs with respect to the original Anisimov *et al.* energy functional¹³ in that it takes into account spin degrees of freedom explicitly for all electrons in the system. Notably, the average occupancy of one d orbital $n^0 = \frac{1}{2(2l+1)} \sum_{m\sigma} n_{m\sigma}$ is now replaced by the spin dependent counterpart $n_{\sigma}^0 = \frac{1}{2l+1} \sum_m n_{m\sigma}$ and the starting energy functional is now the spin polarized LSDA functional, E^S

$$E^U = E^S + \frac{1}{2} \sum_{m,m',\sigma} U(n_{m\sigma} - n_{\sigma}^0)(n_{m'-\sigma} - n_{-\sigma}^0) + \frac{1}{2} \sum_{m \neq m',\sigma} (U - J)(n_{m\sigma} - n_{\sigma}^0)(n_{m'\sigma} - n_{\sigma}^0). \quad (3)$$

Calculations have been performed using the full-potential linearized augmented plane-wave code WIEN2k¹⁴. While the *atomic force* method is more efficient to obtain the dynamical matrix, a successful implementation of this method within LDA+ U is not yet reliable. Here we will present results on the structural properties of TiOCl within LDA considering the *atomic force* method and within LDA+ U by means of the *total energy* method.

Density Functional Calculations.- In our calculations, the expansion of the wave functions included 1207 LAPW's¹⁵ ($RK_{max} = 7$, including 12 Local Orbitals) and the muffin tin radii were chosen to be 1.7 a.u. for Titanium, 1.5 a.u. for Oxygen and 2.00 a.u. for Chlorine. Expansion in spherical harmonics for the radial wave functions were taken up to $l = 10$. Charge densities and potentials were represented by spherical harmonics up to $L = 6$ whereas in the interstitial region they were expanded in a Fourier series with 4500 stars. For Brillouin-zone (BZ) integrations a 500 \mathbf{k} -point mesh was used yielding 60 \mathbf{k} points in the irreducible wedge and use of the modified tetrahedron method was made¹⁶.

Concerning the LDA+ U parameters U and J we have used the values of 4 eV and 1 eV respectively. Here we have considered a larger value of U than in the calculation in ref.⁶($U=3.3\text{eV}$) in line with a Hartree-Fock calculation of on-site Coulomb interaction for transition metal oxides¹⁷.

For a consistent phonon calculation we need to have a well defined *ab initio* equilibrium structure which corresponds to the minimum of the Taylor expansion Eq. 1. Therefore we analyze the structure of TiOCl by performing an atomic position optimization and (within LDA) a unit cell volume optimization. In the volume optimization, the $a : b : c$ ratios were kept constant and equal to the experimental values. For each total energy calculation we allow the ions to relax to their zero-force positions along the c -axis by simulating the dynamics of the damped Newton method. For the time evolution of the three atomic coordinates, the method is based on the

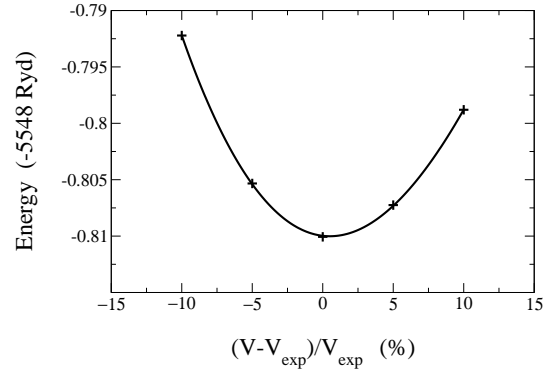


FIG. 1: Volume optimization for TiOCl within LDA with the ratio $a : b : c$ fixed to the experimental one.

TABLE I: Experimental and theoretical structure parameters (z_{Ti} , z_O , z_{Cl} are the c -axis coordinates in units of the c -axis length and the distances Ti-O, Ti-Cl are given in Å).

	z_{Ti}	z_O	z_{Cl}	Ti-O	Ti-O-Ti	Ti-Cl
Exp.	0.1194	0.0551	0.3318	1.96	150°	2.40
LDA	0.0846	0.0724	0.2999	1.89	174°	2.41
LDA+U	0.1133	0.0523	0.3223	1.96	151°	2.38

finite difference equation $z_i^{\tau+1} = z_i^{\tau} + \eta(z_i^{\tau} - z_i^{\tau-1}) + \delta F_i^{\tau}$, where z_i^{τ} and F_i^{τ} are the coordinate and the force on the i -th atom at time step τ . Damping and speed of motion are controlled by the two parameters η and δ respectively.

In Fig. 1 the total energy is displayed versus the volume variation with respect to the experimental reference value. The continuous line represents a fit to the Murnaghan equation of state¹⁸ from which we extract a bulk modulus value of 59.5 GPa. The curve shows that the optimal volume is in good agreement with the experimental one, in contrast with results obtained for high- T_c compounds⁹.

In Table I we show the equilibrium fractional c -axis coordinates, main distances and bonding angle of the three atoms obtained for the optimized lattice parameters. The most important difference with respect to the experimental structure is the shape of the Ti-O chain along the a -axis which in LDA has become almost a linear chain (as shown also by the bonding angle Ti-O-Ti and the contraction of the Ti-O distance).

Recalling that the local Titanium coordinate frame has the z axis parallel to a and the x and y axes rotated by 45° respect to b and c (see Fig. 2), LDA provides a t_{2g} ground state where the d_{xy} and d_{xz} , d_{yz} contributions are comparable in weight (0.2 and 0.27 electrons/eV respectively). On the other hand, the *ab initio* calculations⁶ using the experimental structure indicate that the d_{xy} weight is dominant. The approximate degeneracy of the three t_{2g} orbitals is clearly shown in Fig. 2 where the electron density surface in the energy range -1 eV to E_F for an isovalue of $0.1e/\text{Å}^3$ is drawn and reflects the typical

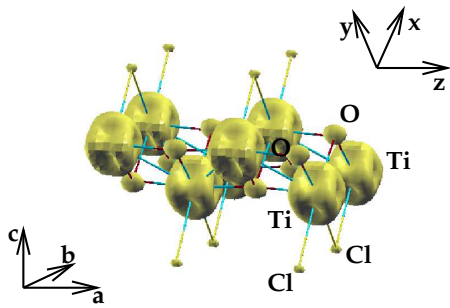


FIG. 2: Electron density surface for an isovalue of $0.1e^{\text{\AA}^3}$ for the LDA equilibrium structure (also shown the global and the local systems of reference).

t_{2g} spatial symmetry with the minima of the isodensity along the octahedron axis. The shortening of the Ti-O distance causes the local octahedron to be more regular and the shape of the surface around the titanium atom to be an equal admixture of d_{xy} , d_{xz} and d_{yz} orbitals.

Turning back to Table I we observe that while the Ti-Cl distance is in good agreement with the experimental one, the Ti-O distance is badly described by the LDA. We ascribe this failure of LDA to the improper description of electron correlations in titanium d -states and we show that inclusion of d -orbital correlations on a mean-field level (LDA+ U) causes the LDA equilibrium structure to be unstable with respect to the experimental one.

In Fig. 3 we present the energy hypersurface in the fractional coordinate space (z_{Ti}, z_O, z_{Cl}) along the line connecting the LDA equilibrium position and the experimental one which is represented approximately by the vector $(z, -z/2, z)$.

It is clear that the inclusion of electron correlations distorts the LDA energy line in a sort of "double-well" curve whose minimum is now very close to the experimental one (see Fig. 3, dotted line). Negative corrections to LDA total energy are expected for partially orbitally polarized LDA groundstates, the amount of which depends on the correlation strength and on the spatial extension of the d orbitals (namely, the U value and the titanium muffin radius). In fact, as shown in Fig 3, the two energy curves match at the LDA equilibrium value of z where an orbitally non-polarized ground state is found.

As a final step in the structure determination of TiOCl we want to find out the equilibrium structure according to the LDA+ U functional. To determine the global minimum of the energy hypersurface we adopt a trial and error approach by performing total energy calculations of all possible distorted structures around the experimental one and obtaining the minimum by a fitting procedure.

As shown in Table I, the experimental distances and bonding angles are well reproduced by the LDA+ U method; the disagreement in this case concerns the absolute fractional coordinates and it results, within every bilayer, in a small reduction of the distance between the two Ti-O layers and accordingly between the outer

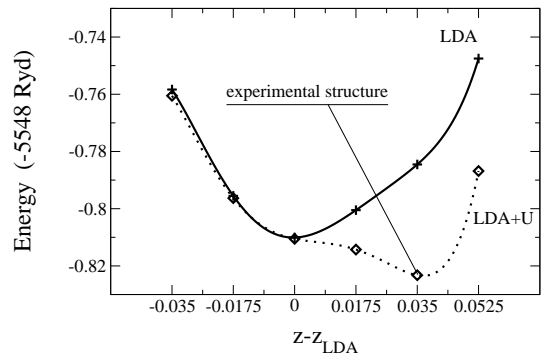


FIG. 3: LDA (solid line) and LDA+ U (dashed line) energy curves along the line $(z, -z/2, z)$ in the space (z_{Ti}, z_O, z_{Cl}) which connects the LDA equilibrium structure (taken as reference) to the experimental one.

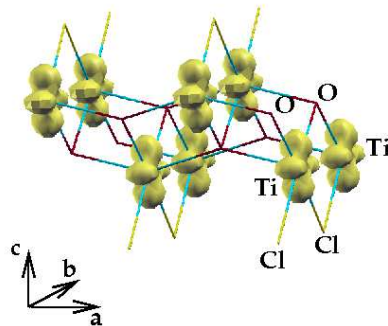


FIG. 4: Electron density surface for an isovalue of $0.1e^{\text{\AA}^3}$ for the LDA+ U equilibrium structure.

Cl ones. In Fig. 4 we show electron density plot of the LDA+ U equilibrium structure at the isosurface $0.1e^{\text{\AA}^3}$.

Preliminary calculations with the Generalized Gradient Approximation¹⁹ (GGA) method show that the optimal equilibrium structure is improved with respect to the LDA results but it is still far from the experimental one.

Phonons within LDA and LDA+ U .- The phonon frequencies within the LDA approximation were calculated by considering the forces acting on the three atoms when they were displaced with respect to the equilibrium positions in all possible fashions (in-phase and out-of-phase displacements of one, two and three atoms). The force values were fitted to linear polynomials in the c -axis coordinates and were determined within the uncertainty of 1 mRy/a.u..

Table II displays the LDA frequencies and the corresponding relative atomic displacements in comparison with the Raman frequencies³. The lowest frequency mode is a titanium-chlorine in-phase and oxygen out-of-phase mode and it shows a considerable disagreement with respect to the experimental value. The second mode is a titanium-oxygen in-phase and chlorine out-of-phase mode and the third mode is mainly given by oxygen with small in-phase contribution of chlorine and almost negligible out-of-phase contribution from titanium. To test

TABLE II: LDA and LDA+ U phonon frequencies compared to experimental data and mode assignment (relative atomic displacement, i.e. components of the eigenvectors divided by $\sqrt{M_i}$ and normalized to the maximum amplitude).

		β	γ	δ
Expt.	freq.(cm ⁻¹)	203	365	430
LDA (mode assign.)	freq.(cm ⁻¹)	154	351	424
	Ti	0.909	0.822	-0.025
	O	-0.157	0.311	1.000
	Cl	1.000	-1.000	0.104
LDA+U (mode assign.)	freq.(cm ⁻¹)	192	336	407
	Ti	0.557	0.307	-0.775
	O	-0.048	1.000	1.000
	Cl	1.000	-0.213	0.614

the accuracy of the fitting polynomials we crosschecked a posteriori the frequency values by displacing the atoms along the eigenvector directions finding the larger deviation ($\sim 10\%$) for the lowest mode.

Within the LDA+ U method we also calculated phonon frequencies and modes by means of a quadratic fitting of total energy surface. The frequencies and assignments are displayed in Table II. The numerical error of the calculation is 10^{-4} Ry and affects mainly the second frequency value. The error due to the fitting function proved to be negligible confirming the harmonic character of all the three vibrations. In LDA+ U the first frequency becomes considerably improved with respect to the LDA value and in good agreement to the experimental mode. The second mode upon inclusion of the numerical error is found in good agreement with the experiment and the third frequency disagrees by about 4%.

Regarding the mode assignments in the two ap-

proaches, both LDA and LDA+ U calculations agree as far as the in-phase and out-of-phase features are concerned. From a quantitative point of view instead, LDA+ U associates in contrast to LDA, a larger amplitude to chlorine and smaller to oxygen in the first mode; in the second mode the principal elongation is the oxygen one with smaller contributions from titanium and chlorine while the latter play the major role in LDA and finally the third mode is characterized by roughly balanced amplitudes for all the three atoms in LDA+ U while in LDA the mode is almost pure oxygen oscillation. Calculation of the Raman cross sections for the three modes would bring to evidence the main differences between the LDA and LDA+ U atomic displacements which can be tested against the experimental Raman intensities.

Conclusions.- Summarizing, we have presented DFT calculations for the A_g Raman phonon modes in TiOCl within LDA and LDA+ U . Within LDA we obtain that the optimized equilibrium structure deviates considerably respect to the experimental one while consideration of electron correlation within the LDA+ U approach brings the DFT minimum very near to the experimental data (importance of correlation effects has been already pointed out by P. Labeguerie *et al.*²⁰ and by M. Merawa *et al.*²¹). In both approaches, by calculation of the dynamical matrix, we obtain the three A_g modes in the $Pmmn$ symmetry. While both LDA and LDA+ U show an overall qualitative agreement with the results from Raman scattering experiments, quantitatively LDA+ U produces for the lower mode the best agreement with the experiment while LDA performs better for the second and third mode.

Acknowledgments.- One of us (L.P.) thanks the WIEN2k-users-web and P. Blaha for useful comments regarding the WIEN2k code and T. Kokalj for providing the graphic code XCRYSDEN. We also thank the German Science Foundation for financial support.

¹ A. Seidel, C. A. Marianetti, F. C. Chou, G. Ceder, and P. A. Lee, Phys. Rev. B **67**, 020405(R) (2003).

² M. Shaz, S. van Smaalen, L. Palatinus, M. Hoinkis, M. Klemm, S. Horn, and R. Claessen *The spin-Peierls transition in TiOCl*, to be published.

³ P. Lemmens, K. Y. Choi, G. Caimi, L. Degiorgi, N. N. Kovaleva, A. Seidel, and F.C. Chou, Phys. Rev. B **70**, 134429 (2004).

⁴ V. Kataev, J. Baier, A. Möller, L. Jongen, G. Meyer, and A. Freimuth, Phys. Rev. B **68**, 140405(R) (2003).

⁵ J. Hemberge, M. Hoinkis, M. Klemm, M. Sing, R. Claessen, S. Horn, and A. Loidl, cond-mat/0501517.

⁶ T. Saha-Dasgupta, R. Valentí, H. Rosner, and C. Gros, Europhys. Lett. **67**, 63 (2004).

⁷ see f. i. W. Cochran, Phys. Rev. Lett. **2**, 495 (1959).

⁸ R. E. Cohen, W. E. Pickett, and H. Krakauer, Phys. Rev. Lett. **62**, 831 (1989).

⁹ R. Kouba and C. Ambrosch-Draxl, and Bernd Zangger,

Phys. Rev. B **60**, 9321 (1999).

¹⁰ J.P. Perdew and Y. Wang, Phys. Rev. B **45**, 13244 (1992).

¹¹ V. Anisimov, F. Aryasetiawan, and A. I. Lichtenstein, J. Phys.: Condens. Matter **9**, 767 (1997).

¹² M.T. Czyzyk and G.A. Sawatzky, Phys. Rev. B **49**, 14211 (1994).

¹³ V.I. Anisimov, J. Zaanen, and O.K. Andersen, Phys. Rev. B **44**, 943 (1991).

¹⁴ P. Blaha, K. Schwarz, G. K. H. Madsen, D. Kvasnicka and J. Luitz, WIEN2k, 2001. ISBN 3-9501031-1-2.

¹⁵ O. K. Andersen, Phys. Rev. B **12**, 3060 (1975).

¹⁶ P.E. Blöchl, O. Jepsen and O.K. Andersen, Phys. Rev B **49**, 16223 (1994)

¹⁷ T. Mizokawa and A. Fujimori, Phys. Rev. B **54**, 5368 (1996).

¹⁸ Murnaghan F.D., Proc.Natl.Acad.Sci. USA **30**, 244 (1944).

¹⁹ J.P. Perdew, K. Burke and M. Ernzerhof, Phys.Rev.Lett. **77**, 3865 (1996).

²⁰ P. Labeguerie, F. Pascale, M. Merawa, C. Zicovich-Wilson,

- N. Makhouki, R. Dovesi, *Eur.Phys.J. B* **43**, 453 (2005).
²¹ M. Merawa, B. Civalleri, P. Ugliengo, Y. Noel, A. Lichanot, *J. Chem. Phys.* **119**, 1045 (2003).